



Silicon surfaces coated with polydopamine and poly (2-hydroxyethyl methacrylate) for medical device applications

Bakhshali Massoumi¹ · Raana Sarvari^{2,3}  · Elaheh Fakhri⁴ · Mehdi Vojoudi Fakhrnezhad¹

Received: 3 October 2023 / Revised: 15 May 2024 / Accepted: 31 May 2024

© The Author(s), under exclusive licence to Springer-Verlag GmbH Germany, part of Springer Nature 2024

Abstract

In order to prevent catheter-associated urinary tract infections caused by biofilm, in this study, polydopamine (PDA) was polymerized in the presence of ammonia on the surface of the silicone samples selected from the urinary catheters used in medicine. The OH groups in polydopamine were alpha-brominated by nucleophilic substitution reaction in the presence of α -bromoisobutyryl bromide. Then, poly (2-hydroxyethyl methacrylate) (PHEMA) was polymerized on the functionalized polydopamine by ATRP polymerization. PHEMA-PDA-coated catheter was evaluated at each step using attenuated total reflection-Fourier transform infrared (ATR-FTIR), scanning electron microscope, thermal gravimetric analysis, and atomic force microscopy, and its hydrophilicity was assessed by water contact angle. The contact angle of water decreases from 115° for uncoated catheter to 84° for PHEMA-PDA-catheter. PHEMA-PDA-coated catheter prevented *Pseudomonas aeruginosa* adhesion and colonization during 24 and 48 h and *Escherichia coli* during 24 h compared to the uncoated sample. It is concluded that functionalization of catheters with PDA-PHEMA appears as a favorable candidate for indwelling urinary catheters.

Keywords PHEMA · Polydopamine · Antibiofilm coating · Hydrogel · Hydrophilicity · Catheter

✉ Raana Sarvari
raanasarvari@yahoo.com; sarvarir@tbzmed.ac.ir

¹ Department of Chemistry, Payam Noor University, Tehran, Iran

² Infectious and Tropical Diseases Research Center, Tabriz University of Medical Sciences, Tabriz, Iran

³ Sarvaran Chemie Pishro Company (S.C.P), Tabriz, Iran

⁴ Dental and Periodontal Research Center, Faculty of Dentistry, Tabriz University of Medical Sciences, Tabriz, Iran

Introduction

Indwelling urinary catheters are used for the long-term management of patients with chronic urinary retention since intermittent catheterization requires frequent surgeries and imposes a great discomfort on patient [1, 2]. Infection and encrustation are the common complications that may arise in patients with urinary catheterization, and importantly, patients with indwelling catheters have higher chances of asymptomatic bacteriuria [3]. Preventive strategies have been suggested against catheter-associated urinary tract infections in hospital care units; however, development of antifouling and antibiofilm catheter coatings is a practical way to address this issue [4].

Urinary catheters are usually based on flexible hydrophobic polymeric materials such as silicone rubber or polyurethane; however, such materials provide breeding surfaces for urinary pathogens to adhere, colonize and form an extracellular polymeric substance named biofilm. Common uropathogens including gram-negative (*Pseudomonas aeruginosa*, *Escherichia coli* and *Klebsiella pneumoniae*) and gram-positive bacteria (*Staphylococcus aureus*) are involved in catheter-related urinary tract infections, which account for about 9% of hospital-acquired infections while almost 65–70% of them are preventable [5–7].

The most common interventions against catheter-related urinary tract infections are catheter replacement or antibiotic therapy, which inevitably leads to the emergence of drug-resistant bacteria. Long-term antibiotic therapy thrust a strong economic and biological burden worldwide and intermittent catheterization imposes high discomfort and frequent surgeries and costs a lot for the patients [8]. Surface modification of catheters to prevent bacteria accumulation and consequently inhibit microbial colonization has been recognized as a solution [9].

In general, surface modification of catheters is often done by three strategies: development of anti-adhesive or antifouling coating, antibacterial coating or a combination of both [10]. The microbial adhesion to the silicon surface is a mechanism involving the physicochemical properties of surface and the microorganism. In particular, the anti-adhesive coatings are designed to resist the bacteria and protein adsorption. These coatings are well-hydrated hydrophilic polymers such as poly (ethylene glycol) (PEG) or polyzwitterionic materials that interfere with the bacteria and protein adhesion by formation of a hydrated layer, which acts as a physical and energetic barrier without biocidal effect. In contrast, the bioactive antibacterial coatings exert their effects by releasing a loaded antibacterial agent over time in order to kill bacteria or limit their growth on the surface of the coating [11–15].

To overcome limitations of catheter's hydrophobic polymers, coating hydrogel materials can be employed due to their well-established tissue compatibility. Hydrogels are a group of three-dimensional (3D) cross-linked polymer networks, which can absorb and imbibe large amounts of water when fully swollen [16]. These materials are insoluble and present solid-like characteristics that provide desirable increased mechanical strength properties [17]. As mentioned above, hydrogels present the essential properties as anti-adhesive catheter coatings.

Along with swelling, hydrogels create a hydrophilic layer with low friction coefficient on the surface of the catheter, which prevents the absorption of proteins and biofilm formation [18–20]. Biocompatible and non-degradable PHEMA hydrogels are materials used widely in the tissue engineering such as cartilage substitutes, orbital implants, bone tissue regeneration and coating medical devices [21, 22]. PHEMA-based hydrogels exhibit superior cytocompatibility, high oxygen permeability, stability and acceptable mechanical strength [23, 24].

Although various modifications of urinary catheter wall surface for reduction of bacteria adherence and colonization and prevention of encrustation have been reported in the literature, research for development of durable antimicrobial catheters is still ongoing. In this regard, this study aimed to propose a new practical method for implementation of PHEMA hydrogel coating on silicon catheters and evaluated its various physical and antibacterial activities.

Materials and methods

Materials

Dopamine was prepared from Sigma-Aldrich (USA) and used without any purification. HEMA (Merck, Darmstadt, Germany) was dried over calcium hydride, vacuum-distilled and then stored at $-20\text{ }^{\circ}\text{C}$ prior to application. Copper (I) chloride (CuCl) was obtained from Sigma-Aldrich and was purified by stirring in acetic acid, then washed with ethanol and dried under vacuum. α -Bromoisobutyryl bromide (BIBB) and N, N, N', N'', N''' -pentamethyldiethylenetriamine (PMDETA) were purchased from Merck. All other reagents were purchased from Merck and purified according to standard methods.

Dopamine polymerization on catheter

Dopamine was polymerized on silicon in the presence of ammonia. For this purpose, pieces of silicone were placed into a solution of water and ethanol 30% (v/v) and the pH of solution was adjusted between 9 and 10 by increasing the amount of ammonia. Then, dopamine was added to the prepared mixture and it was stirred for 24 h under a magnetic stirrer at room temperature. The obtained product was washed several times with water and ethanol separately and dried.

Functionalization of catheter-PDA with ATRP initiator

PDA-coated catheter pieces were placed into a 100-mL three-neck round-bottom flask and then, triethylamine was added to the flask along with 25 mL of dry dichloromethane. The system was placed in an ice bath. While the reaction mixture was under N_2 gas, its temperature was brought to $0\text{ }^{\circ}\text{C}$. On the other hand, in another suitable container, BIBB was poured in 10 mL of dichloromethane and slowly entered the flask. After transferring the solution containing the ATRP reagent, the

system was completely closed and stirred at room temperature for 24 h under N₂ gas. Precipitation of triethylamine hydrobromide took place during the reaction. After the completion of the reaction, the coated catheters were separated from the contents of the flask and washed several times with dichloromethane and dried.

Polymerization of HEMA on PDA-catheter

The polymerization of HEMA was carried out on the functionalized PDA-catheter. Specimens were placed into a 100-mL three-neck round-bottom flask, 2-hydroxyethyl methacrylate monomer, CuCl, and PMDETA were added at a ratio of 100/1/2, and 10 mL of dimethylformamide (DMF) was added. The contents of the container were degassed by N₂ gas for several minutes. Then, the flask was placed in an oil bath with a temperature of 70 °C. The reaction mixture was stirred for 24 h. After this period, in order to stop the polymerization, the temperature of the reaction was quickly lowered to 4 °C. The obtained catheters were washed several times with water and methanol.

Antibacterial activity

Escherichia coli (ATCC 25922) and *Pseudomonas aeruginosa* (ATCC 27853) strains were subcultured on Mueller–Hinton agar plates (Merck, Darmstadt, Germany) and then incubated at 37 °C for 24 h at 37 °C. Single colonies of each bacterium were suspended in trypticase soy broth (TSB and 1% glucose) (Merck, Darmstadt, Germany), incubated at 37 °C for 24 h and were diluted to a turbidity of 5×10^5 colony-forming unit [CFU]/mL using a spectrophotometer. Specimens were placed in a 48-well microplate, inoculated with 1 mL of bacterial suspension and incubated for 24 or 48 h at 37 °C under 50 rpm rotation. The inoculum was removed, and the density of the microbial broth culture was determined by plating 10 µL of serially diluted inoculum on agar plates. To evaluate the antibiofilm activity, catheter samples were rinsed gently with the sterile phosphate-buffered solution for 1 min to remove unattached bacterial cells and then placed in sterile micro-tubes containing 1 mL of PBS and vortexed for 1 min. The suspensions were serially diluted, and then, 10 µL of each dilution was suspended on Mueller–Hinton agar plates and incubated at 37 °C and 5% CO₂ for 24 h. After incubation, the colony-forming units (CFU/mL) were calculated [25].

Cell viability

L929 mouse fibroblast cell line was employed in the cytotoxicity test. The Dulbecco's Modified Eagle's Medium (Gibco; Thermo Fisher Scientific, Inc., Waltham, MA, USA) containing 10% of fetal bovine serum (Gibco; Thermo Fisher Scientific, Inc., Waltham, MA, USA) and 100 U mL⁻¹ Penicillin/Streptomycin (Gibco; Thermo Fisher Scientific, Inc., Waltham, MA, USA) was used as the culture medium. Briefly, functionalized and simple silicon pieces were placed into 48-well plates. Then, cells were seeded on the specimens at a density of 10⁵ cells/well and

incubated at 37 °C with 5% CO₂ for 24, 48 and 72 h. After the incubation, the supernatant culture medium was removed and cells were gently washed with phosphate buffer saline 3 times. In the next step, 3-(4,5-dimethylthiazol-2-yl)-2,5-diphenyl tetrazolium bromide (MTT) solution was added and plates were incubated for 4 h. The intracellular formazan crystals were dissolved following the addition of dimethyl sulfoxide (DMSO). Ultimately, the absorbance of the suspension was measured at 570 nm.

Characterization

The surface morphology of samples was characterized using FESEM type 1430 VP (LEO Electron Microscopy Ltd, Cambridge, UK) under vacuum at room temperature, and the 3D exploration of the samples' surface was conducted by AFM (*Nano-Surf Core AFM*, Nanosurf AG, Liestal, Switzerland). In order to identify the functional groups of samples, FTIR spectra (Shimadzu, Japan) were obtained at room temperature under ATR mode in the range from 400 to 4000 cm⁻¹. TGA was conducted in the temperature range of 25–700 °C at a heating rate of 10 °C min⁻¹ under a N₂ atmosphere. The wettability of the catheters was measured via the drop water contact angle measurement using an OCA 20 plus contact angle meter system (Data Physics Instruments GmbH, Filderstadt, Germany).

Result and discussion

Catheter-associated urinary tract infections are one of the most common health care acquired infections, and the possibility of development of bacteremia is high among patients with indwelling catheters. Permanent implanted catheters are susceptible to bacterial adhesion, proliferation, biofilm formation and as a result, infection [26]. The greatest part of the materials used in the production of catheters are hydrophobic and consequently present low lubricity, high surface friction between urethra and catheter and weak antibacterial properties. The large frictional forces lead to friction between catheters and urethra and result in tissue damage following by bacterial colonization and infection. Hydrogel-coated catheters present lubrication to reduce the urethra tissue damages and antiprotein adsorption and antifouling activities [27]. In the present research work, in order to modify the surface of silicone rubber, dopamine was polymerized on silicon in the presence of ammonia, and in the next step, the hydroxyl groups on polydopamine were functionalized by BIBB and then HEMA by ATRP polymerization was polymerized on PDA (Fig. 1).

ATFT-IR

FT-IR spectra of uncoated catheter and PDA-coated catheter are presented in Fig. 2a, b. In the spectrum of uncoated catheter (Fig. 2a), two stretching vibrations at 1009 and 1075 cm⁻¹ are related to the Si–O–Si bond and the bending vibration at 787 cm⁻¹ is attributed to the Si–OH bond. In the ATFT-IR spectrum

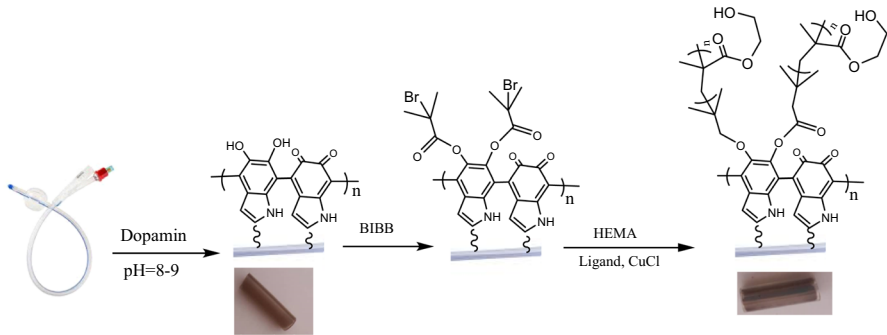


Fig. 1 Schematic illustration of catheter coating

of catheter coated with PDA (Fig. 2b), a broad band can be seen in the region of 3422 cm^{-1} , which is related to the stretching vibrations of the OH– hydroxyl group. The intensity of this band confirms the PDA covering. The observed band at 1258 cm^{-1} , 3052 cm^{-1} and the bands observed at 1651 and 1470 cm^{-1} are related to the C–N stretching vibrations, the aromatic C–H group stretching vibrations and the C=C stretching vibrations of the aromatic ring of dopamine [28]. Therefore, the binding of PDA on catheter is confirmed.

The FT-IR spectrum of PDA-catheter functionalized by BIBB is shown in Fig. 2c. The weakening of the OH broad band related to PDA demonstrates the binding of BIBB. As it is clear, all the bands related to PDA and catheter can be seen in this spectrum, and unfortunately, it overlaps with some absorption bands of BIBB, including the C–O band of the ester group and C–Br. The stretching vibrations related to carbonyl at 1731 cm^{-1} and the absorption bands related to the C–O bond of the ester group at 1011 and 1031 cm^{-1} overlap with Si–O–Si bands of catheter. Furthermore, aromatic C–H bonds are seen in the region of 3050 cm^{-1} and aromatic C=C stretching vibrations are seen in 1470 and 1650 cm^{-1} . The broad band of hydroxyl groups can be seen in the region of 3424 cm^{-1} . By comparing the two graphs of catheter coated with non-functionalized PDA in Fig. 2b, c, it is clear that the intensity of the band of hydroxyl groups is weaker, so the functionalization of PDA by BIBB is confirmed.

The FT-IR spectrum related to the polymerization of HEMA is presented in Fig. 2d. The absorption bands observed in activated polydopamine can also be seen in this spectrum. A slight difference can be seen only in the absorption intensity and wave numbers. The basic difference that confirms the polymerization of HEMA is the increase in the intensity of the broad band related to O–H. The rest of the bands corresponding to PHEMA overlap with the previous bands [29]. Moreover, by comparing the graphs, it is evident that the band of hydroxyl groups related to HEMA has become more intense. Therefore, the polymerization of HEMA is confirmed.

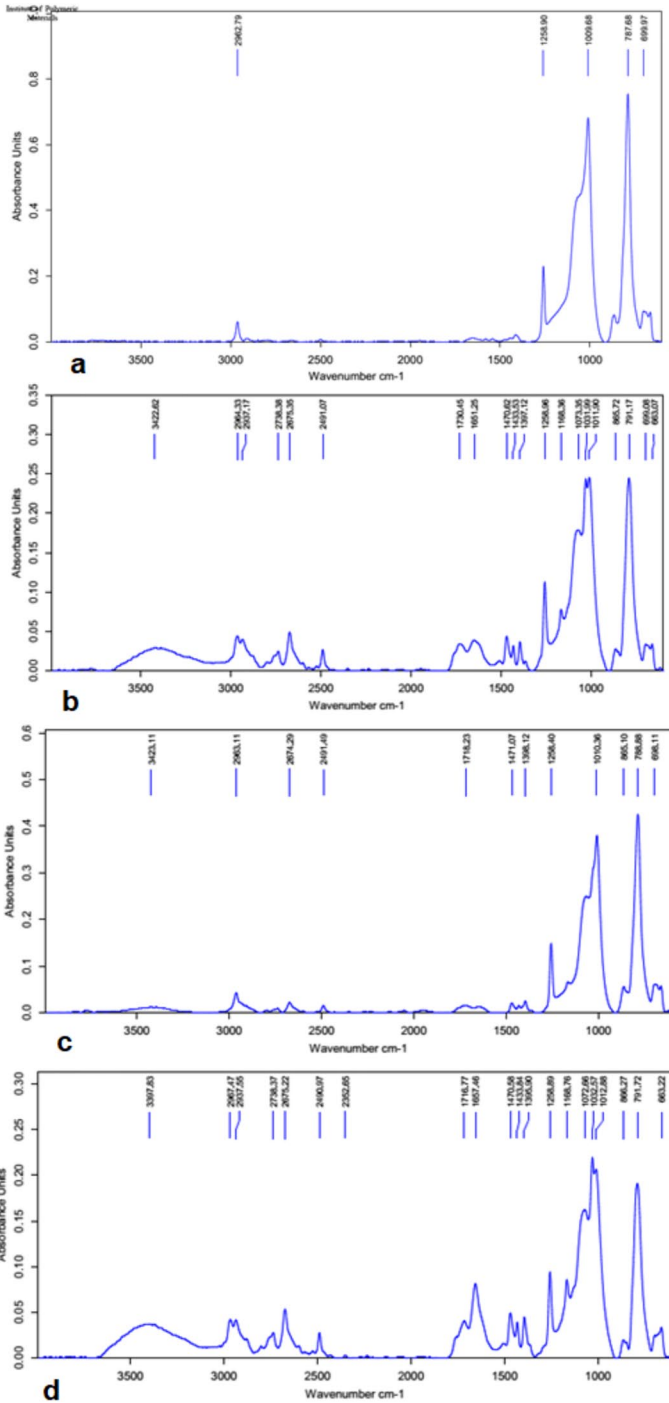


Fig. 2 ATFT-IR spectrum of catheter (a), PDA-catheter (b), Br-PDA-catheter (c), and PHEMA-PDA-catheter (d)

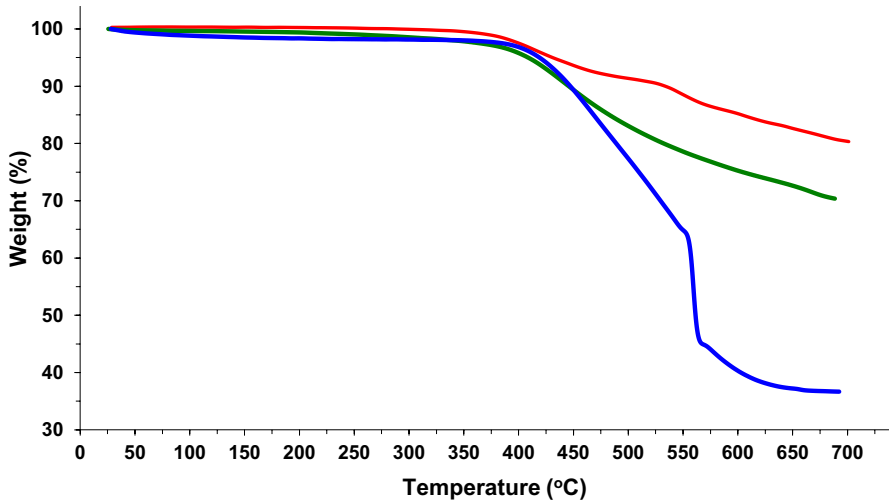


Fig. 3 TGA curves of catheter (red), PDA-catheter (green), and PHEMA-PDA-catheter (blue) (color figure online)

Thermal stability

TGA curves of catheter, PDA-catheter, and PHEMA-PDA-catheter are shown in Fig. 3. All three samples present thermal stability up to 440 °C and all samples lost weight at higher temperatures. The uncoated catheter has less weight loss at 700 °C since it has retained about 80% of its weight. While the catheter coated with polydopamine (Fig. 3) and the catheter coated with PDA-PHEMA (Fig. 3) demonstrate a greater weight loss, suffer degradation up to 30% and 74%, and kept approximately 70% and 36% of their weight at 700 °C. As expected, the graph of the sample coated with PDA-PHEMA shows a steeper weight loss at 555 °C, which can be related to the degradation of PHEMA and indicates the successful polymerization of PHEMA on PDA-catheter.

SEM

SEM images of catheter (a), PDA-catheter (b), PDA-catheter functionalized by BIBB (c) and PHEMA-PDA-catheter (d) are shown in Fig. 4. As can be seen in Fig. 4a, catheter surface is completely smooth without any kinds of coating. According to Fig. 4b, c, a uniform polydopamine coating is developed on the catheter surface, which is in the form of spherical grains. Comparing the SEM images of PDA-catheter with PHEMA-PDA-catheter, it can be seen that the specific grains shown in Fig. 4b, c are covered in Fig. 4d and these changes confirm the growth of PHEMA on PDA. The EDS analysis showed the elemental composition of catheters in various coating stages. According to Fig. 5, by increasing the coating thickness, the amount of silicon decreases and carbon increases. The appearance of nitrogen in second figure is due to the amine groups of dopamine.

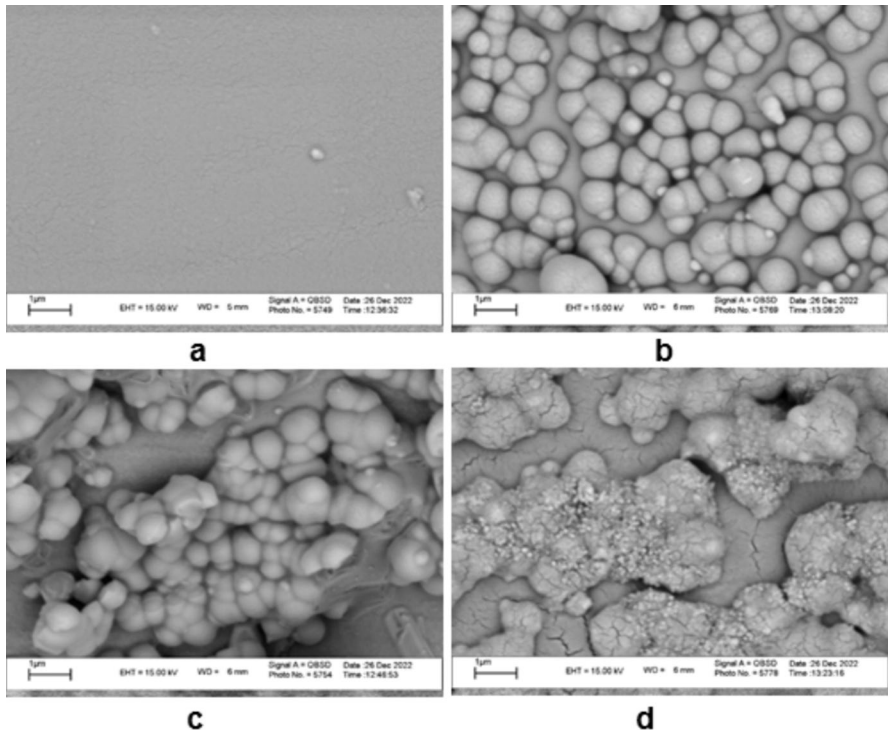


Fig. 4 SEM images of catheter (a), PDA-catheter (b), Br-PDA-catheter (c), and PHEMA-PDA-catheter (d)

AFM

AFM images of catheter (a), PDA-catheter (b), and PHEMA-PDA-catheter (c) are shown in Fig. 6. The morphology of the uncoated catheter has completely undergone significant changes following the PDA and PHEMA coatings. The uniform surface of catheter in Fig. 5a can be seen, and with polymerization of dopamine on it, a uniform surface but different from the uncoated catheter has been created. These morphological changes observed in the images are completely consistent with the results obtained from SEM. In these images, PDA coating showed a non-flat and granular surface, and with the polymerization of HEMA, the surface morphology was somewhat flat. On the other hand, the changes in each of these images confirm the different coatings created to modify the catheter surface.

Contact angle

The images related to the contact angle of the water drop with uncoated and coated catheter samples are shown in Fig. 7. The results show that the uncoated catheter

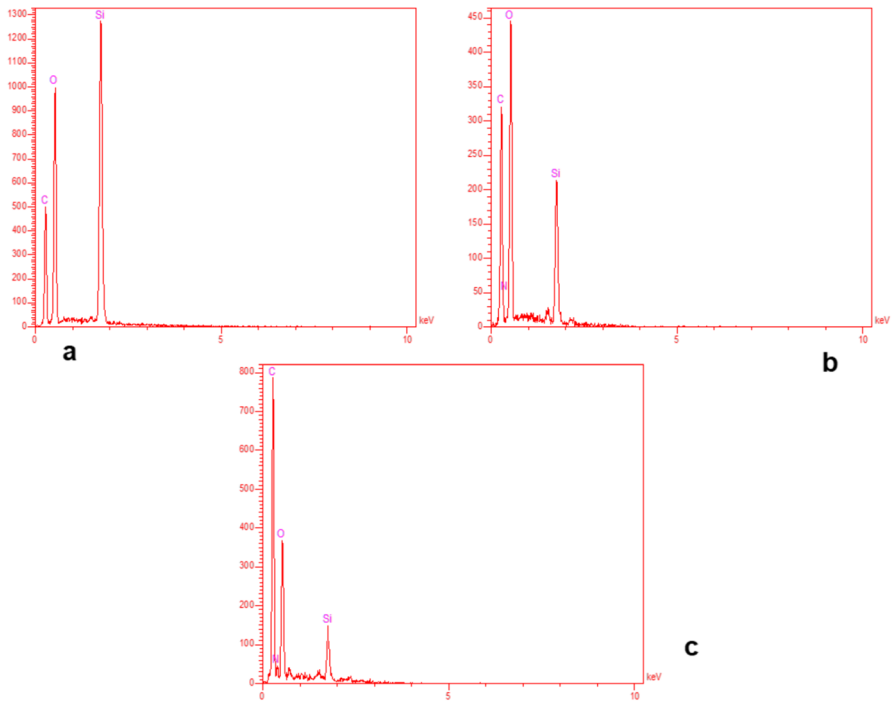


Fig. 5 EDS images of catheter (a), PDA-catheter (b), and PHEMA-PDA-catheter (c)

surface is hydrophobic, and with the polydopamine and PHEMA coating, the contact angle of water decreases from 115° for uncoated catheter to 84° for PHEMA-PDA-catheter. This demonstrates the hydrophilic structure of polydopamine and PHEMA coatings. Previous studies also showed that PHEMA coatings increase the wettability noticeably [29]. It has been acknowledged that microstructuring the catheter surface alters the surface wettability, affecting cell adhesion, proliferation and ultimately colonization [30, 31]. The higher water retention and wettability of PHEMA-PDA-catheter indicate the improved lubricating performance of developed catheter.

Antibacterial properties

It has been reported that *P. aeruginosa*, *E. coli*, *S. aureus* and *P. mirabilis* are commonly detected in urinary tract infections [2, 7]. Catheter coatings with intrinsic antibacterial effects or anti-adhesive activities have been introduced to reduce the urinary tract infections prevalence. In this study, coated catheters at each stage were investigated for antibacterial activities against the growth of *P. aeruginosa* and *E. coli* in planktonic and biofilm states at 24 and 48 h of incubation with the tested samples. The reason the emphasis was on Gram-negative pathogens in this study is the lipopolysaccharide outer membrane of

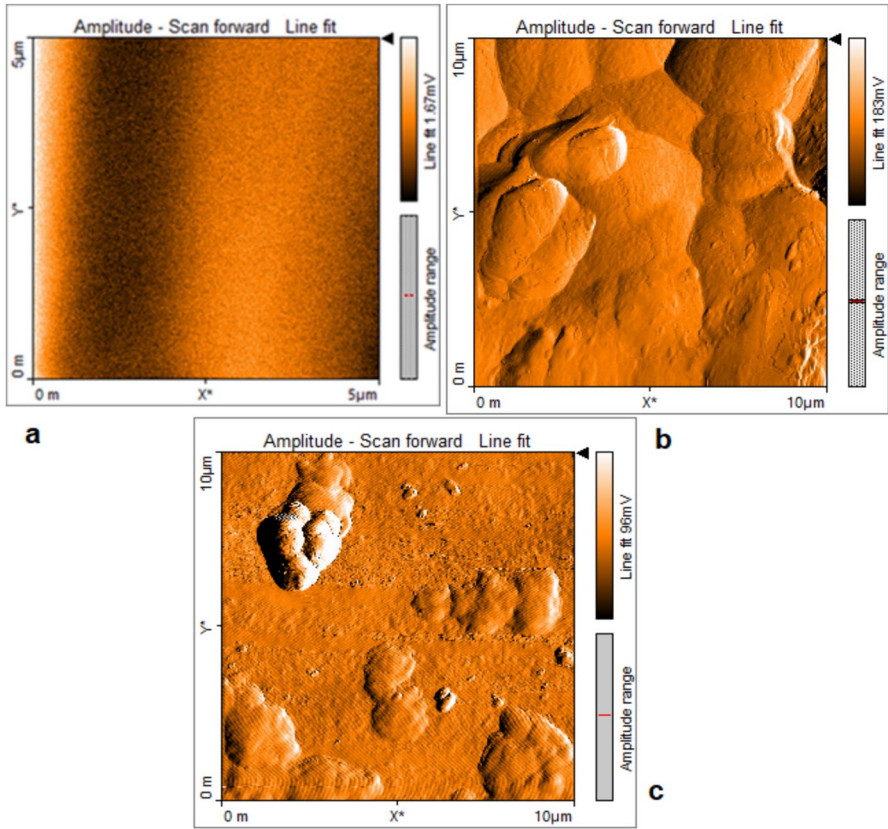


Fig. 6 AFM images of catheter (a), PDA-catheter (b), and PHEMA-PDA-catheter (c)

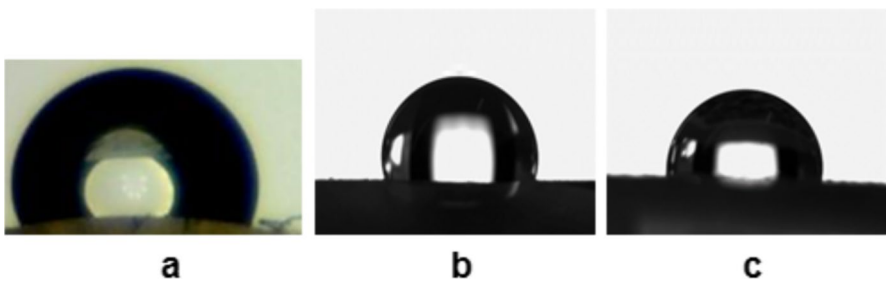


Fig. 7 Water contact angles of catheter (a), PDA-catheter (b), and PHEMA-PDA-catheter (c)

these bacteria that resists against most of recently developed antibiotics resulting in the growing threat of drug resistance [32, 33]. The antibacterial properties against *P. aeruginosa* and *E. coli* in planktonic and biofilm forms are shown in Fig. 8. The uncoated, PDA-coated and PHEMA-PDA-coated samples did not demonstrate antibacterial activity in planktonic bacterial growth state. This

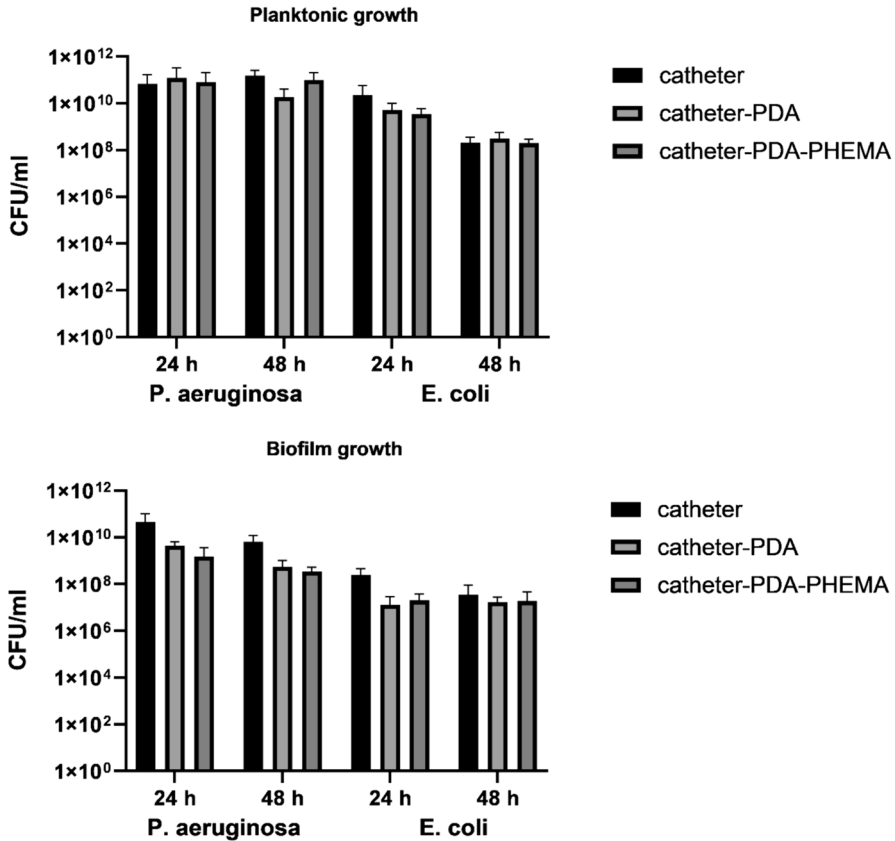


Fig. 8 The number of viable bacterial cells (CFU/mL) for catheter (control), PDA-catheter, PHEMA-PDA-catheter against *P. aeruginosa* and *E. coli* in planktonic and biofilm forms

result is due to the strategy employed in this study against urinary tract infections, which was to develop an anti-adhesive or antifouling coating. Notwithstanding, the highly hydrophilic nature of the PHEMA-PDA-coated catheter surface impeded the bacterial cells' adhesion and impaired the biofilm formation of both *P. aeruginosa* and *E. coli* during 24 and 48 h. PHEMA-PDA-coated catheter prevented *P. aeruginosa* adhesion and colonization during 24 and 48 h and *E. coli* during 24 h compared to the uncoated sample. Hydrogel PHEMA-coated catheters demonstrated inhibitory effects against *P. aeruginosa* attachment due to the anti-adhesive polymer chains [11]. As previous studies demonstrated, PHEMA-coated catheters present low antibacterial activity [34], however, addition of PDA was helpful in increasing this characteristic. In this study, biofilm thickness was evaluated by counting colony forming units on catheter samples which decreased on PDA-coated and PHEMA-PDA-coated ones compared to the uncoated silicon catheter.

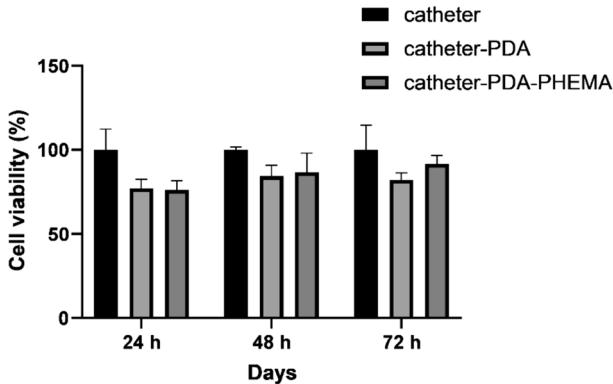


Fig. 9 Biocompatibility of catheter, PDA-catheter, and PHEMA-PDA-catheter with fibroblast cell line

Biocompatibility

In order to investigate the cytotoxicity of developed coatings, L929 fibroblast cells were incubated on uncoated and coated catheters for 24, 48, and 72 h and the cell viability was assessed using the MTT method (Fig. 9). The results showed that despite a slight decrease in cell proliferation on coated catheters during the first 24 h, the PDA-catheter and final coated catheter (PHEMA-PDA-catheter) presented an acceptable cytocompatibility after 72 h and the mean cell viability was over 80% and 90%, respectively.

Conclusion

In this work, a hydrophilic coating based on PDA and PHEMA hydrogel is developed on silicon catheters and the results show that compared to the uncoated samples, PHEMA-PDA-catheter has a lower contact angle and is more hydrophilic. This characteristic leads to antifouling characteristic of the coated catheter. PHEMA-PDA-coated catheter prevented *P. aeruginosa* adhesion and colonization during 24 and 48 h and *E. coli* during 24 h compared to the uncoated sample. Hydrogel PHEMA-coated catheters demonstrated inhibitory effects against *P. aeruginosa* attachment due to the anti-adhesive polymer chains. The fabricated hydrogel coating was biocompatible with L929 fibroblast cells during 72 h. It is concluded that the PHEMA-PDA-coated catheter possesses the potentiality to be a step to solve the urinary silicon catheter lubricity and infections and the results of this study support further clinical investigations.

Acknowledgements Financial support from Payame Noor University is gratefully acknowledged.

Declarations

Conflict of interest The authors declare that they have no conflict of interest.

References

- Feneley RC, Kunin CM, Stickler DJ (2012) An indwelling urinary catheter for the 21st century. *BJU Int* 109(12):1746–1749. <https://doi.org/10.1111/j.1464-410X.2011.10753.x>
- Ramadan R et al (2021) Bacterial biofilm dependent catheter associated urinary tract infections: characterization, antibiotic resistance pattern and risk factors. *Egypt J Basic Appl Sci* 8(1):64–74. <https://doi.org/10.1080/2314808X.2021.1905464>
- Kidd EA et al (2015) Urethral (indwelling or intermittent) or suprapubic routes for short-term catheterisation in hospitalised adults. *Cochrane Database Syst Rev* 2015(12):cd004203. <https://doi.org/10.1002/14651858.CD004203.pub3>
- Andersen MJ, Flores-Mireles AL (2019) Urinary catheter coating modifications: the race against catheter-associated infections. *Coatings* 10(1):23. <https://doi.org/10.3390/coatings10010023>
- Magill SS et al (2014) Multistate point-prevalence survey of health care-associated infections. *N Engl J Med* 370(13):1198–1208. <https://doi.org/10.1056/NEJMoa1306801>
- Umscheid CA et al (2011) Estimating the proportion of healthcare-associated infections that are reasonably preventable and the related mortality and costs. *Infect Control Hosp Epidemiol* 32(2):101–114. <https://doi.org/10.1086/657912>
- Almalki MA, Varghese R (2020) Prevalence of catheter associated biofilm producing bacteria and their antibiotic sensitivity pattern. *J King Saud Univ Sci* 32(2):1427–1433. <https://doi.org/10.1016/j.jksus.2019.11.037>
- Nicolle LE (2014) Catheter associated urinary tract infections. *Antimicrob Resist Infect Control* 3:1–8. <https://doi.org/10.1186/2047-2994-3-23>
- Anjum S et al (2018) Biomodification strategies for the development of antimicrobial urinary catheters: overview and advances. *Global Chall* 2(1):1700068. <https://doi.org/10.1002/gch2.201700068>
- Zhu Z et al (2019) Antimicrobial strategies for urinary catheters. *J Biomed Mater Res A* 107(2):445–467. <https://doi.org/10.1002/jbm.a.36561>
- Neoh KG et al (2017) Surface modification strategies for combating catheter-related complications: recent advances and challenges. *J Mater Chem B* 5(11):2045–2067. <https://doi.org/10.1039/C6TB03280J>
- Sarvari R et al (2023) Organic/polymeric antibiofilm coatings for surface modification of medical devices. *Int J Polym Mater* 72(11):867–908. <https://doi.org/10.1080/00914037.2022.2066668>
- Yu H et al (2007) Preparation and antibacterial effects of PVA-PVP hydrogels containing silver nanoparticles. *J Appl Polym Sci* 103(1):125–133. <https://doi.org/10.1002/app.24835>
- Abdali K et al (2022) Morphological, optical, electrical characterizations and anti-escherichia coli bacterial efficiency (AECBE) of PVA/PAAm/PEO polymer blend doped with silver NPs. *Nano Biomed Eng* 14(2):114–122. <https://doi.org/10.5101/nbe.v14i2.p114-122>
- Kadim AM et al (2024) Effect of loading corn starch nanoparticles on the morphological, optical, and dielectric behaviors of PVA/PMMA/PAAm polymer blend for optoelectronic and antibacterial applications. *Nano Biomed Eng* 16(1):119–127. <https://doi.org/10.26599/NBE.2024.9290049>
- Ahmed EM (2015) Hydrogel: preparation, characterization, and applications: a review. *J Adv Res* 6(2):105–121. <https://doi.org/10.1016/j.jare.2013.07.006>
- Jafari B, Rafie F, Davaran S (2011) Preparation and characterization of a novel smart polymeric hydrogel for drug delivery of insulin. *Bioimpacts* 1(2):135. <https://doi.org/10.5681/bi.2011.018>
- Moureau N (2024) Hydrophilic biomaterial intravenous hydrogel catheter for complication reduction in PICC and midline catheters. *Expert Rev Med Devices* 21(3):207–216. <https://doi.org/10.1080/17434440.2024.2324885>
- Sun C et al (2024) Fast-polymerized lubricant and antibacterial hydrogel coatings for medical catheters. *J Chem Eng* 488:150944. <https://doi.org/10.1016/j.cej.2024.150944>
- Yong Y et al (2018) Conformal hydrogel coatings on catheters to reduce biofouling. *Langmuir* 35(5):1927–1934. <https://doi.org/10.1021/acs.langmuir.8b03074>

21. Zare M et al (2021) pHEMA: an overview for biomedical applications. *Int J Mol Sci* 22(12):6376. <https://doi.org/10.3390/ijms22126376>
22. Fathi M et al (2015) Hydrogels for ocular drug delivery and tissue engineering. *Bioimpacts* 5:159–164. <https://doi.org/10.15171/bi.2015.31>
23. Passos M et al (2016) pHEMA hydrogels: synthesis, kinetics and in vitro tests. *J Therm Anal Calorim* 125:361–368. <https://doi.org/10.1007/s10973-016-5329-6>
24. Saraei M et al (2019) Co-delivery of methotrexate and doxorubicin via nanocarriers of star-like poly (DMAEMA-block-HEMA-block-AAc) terpolymers. *Polym Int* 68(10):1795–1803. <https://doi.org/10.1002/pi.5890>
25. Badica P et al (2021) Antibacterial composite coatings of MgB₂ powders embedded in PVP matrix. *Sci Rep* 11(1):9591. <https://doi.org/10.1038/s41598-021-88885-2>
26. Percival SL et al (2015) Healthcare-associated infections, medical devices and biofilms: risk, tolerance and control. *J Med Microbiol* 64(4):323–334. <https://doi.org/10.1099/jmm.0.000032>
27. Dai S, Gao Y, Duan L (2023) Recent advances in hydrogel coatings for urinary catheters. *J Appl Polym Sci* 140(14):e53701. <https://doi.org/10.1002/app.53701>
28. Yassin MA et al (2019) Facile coating of urinary catheter with bio-inspired antibacterial coating. *Heliyon* 5(12):e02986. <https://doi.org/10.1016/j.heliyon.2019.e02986>
29. Indolfi L, Causa F, Netti PA (2009) Coating process and early stage adhesion evaluation of poly (2-hydroxy-ethyl-methacrylate) hydrogel coating of 316L steel surface for stent applications. *J Mater Sci Mater Med* 20(7):1541–1551. <https://doi.org/10.1007/s10856-009-3699-z>
30. Gallarato LA et al (2017) Synergistic effect of polyaniline coverage and surface microstructure on the inhibition of pseudomonas aeruginosa biofilm formation. *Colloids Surf B Biointerfaces* 150:1–7. <https://doi.org/10.1016/j.colsurfb.2016.11.014>
31. Keyhanvar N et al (2022) The combined thermoresponsive cell-imprinted substrate, induced differentiation, and “KLC sheet” formation. *Adv Pharm Bull* 12(2):356
32. Lam SJ et al (2016) Combating multidrug-resistant Gram-negative bacteria with structurally nano-engineered antimicrobial peptide polymers. *Nat Microbiol* 1(11):1–11. <https://doi.org/10.1038/nmicrobiol.2016.162>
33. Lewis K (2013) Platforms for antibiotic discovery. *Nat Rev Drug Discov* 12(5):371–387. <https://doi.org/10.1038/nrd3975>
34. Xu T et al (2018) A poly (hydroxyethyl methacrylate)–Ag nanoparticle porous hydrogel for simultaneous in vivo prevention of the foreign-body reaction and bacterial infection. *Nanotechnol* 29(39):395101. <https://doi.org/10.1088/1361-6528/aad257>

Publisher's Note Springer Nature remains neutral with regard to jurisdictional claims in published maps and institutional affiliations.

Springer Nature or its licensor (e.g. a society or other partner) holds exclusive rights to this article under a publishing agreement with the author(s) or other rightsholder(s); author self-archiving of the accepted manuscript version of this article is solely governed by the terms of such publishing agreement and applicable law.